

Report

The Yeast Polo Kinase Cdc5 Regulates the Shape of the Mitotic Nucleus

Alison D. Walters,¹ Christopher K. May,¹ Emma S. Dauster,¹ Bertrand P. Cinquin,^{2,3} Elizabeth A. Smith,^{2,3} Xavier Robellet,⁴ Damien D'Amours,⁴ Carolyn A. Larabell,^{2,3} and Orna Cohen-Fix^{1,*}

¹Laboratory of Molecular and Cellular Biology, National Institute of Diabetes and Digestive and Kidney Diseases, NIH, Bethesda, MD 20892, USA

²Department of Anatomy, University of California, San Francisco, San Francisco, CA 94158, USA

³Physical Biosciences Division, Lawrence Berkeley National Laboratory, Berkeley, CA 94720, USA

⁴Institute for Research in Immunology and Cancer and Département de Pathologie et Biologie Cellulaire, Université de Montréal, Montréal, QC H3C 3J7, Canada

Summary

Abnormal nuclear size and shape are hallmarks of aging and cancer [1, 2]. However, the mechanisms regulating nuclear morphology and nuclear envelope (NE) expansion are poorly understood. In metazoans, the NE disassembles prior to chromosome segregation and reassembles at the end of mitosis [3]. In budding yeast, the NE remains intact. The nucleus elongates as chromosomes segregate and then divides at the end of mitosis to form two daughter nuclei without NE disassembly. The budding yeast nucleus also undergoes remodeling during a mitotic arrest; the NE continues to expand despite the pause in chromosome segregation, forming a nuclear extension, or “flare,” that encompasses the nucleolus [4]. The distinct nucleolar localization of the mitotic flare indicates that the NE is compartmentalized and that there is a mechanism by which NE expansion is confined to the region adjacent to the nucleolus. Here we show that mitotic flare formation is dependent on the yeast polo kinase Cdc5. This function of Cdc5 is independent of its known mitotic roles, including rDNA condensation. High-resolution imaging revealed that following Cdc5 inactivation, nuclei expand isometrically rather than forming a flare, indicating that Cdc5 is needed for NE compartmentalization. Even in an uninterrupted cell cycle, a small NE expansion occurs adjacent to the nucleolus prior to anaphase in a Cdc5-dependent manner. Our data provide the first evidence that polo kinase, a key regulator of mitosis [5], plays a role in regulating nuclear morphology and NE expansion.

Results and Discussion

Cdc5 Affects Nuclear Morphology during a Mitotic Arrest

During interphase, nuclei of budding yeast are typically round, with the nucleolus forming a crescent-shaped mass at the nuclear periphery (Figure 1A). During a mitotic delay the nuclear envelope (NE) continues to expand, forming an extension, or flare, that encompasses the nucleolus (Figure 1A) [4]. Whereas in interphase the interface between the nucleolus and the rest of the nucleoplasm is extensive (Figure 1A, image 1, arrowhead), in the flare the nucleolus has only a very narrow interface

with the rest of the nucleoplasm (Figure 1A, image 2, arrowhead). To understand this spatially restricted NE expansion, we screened for mutants that maintain a round nucleus when arrested in mitosis. Because flare formation may occur through the same process that normally drives NE expansion, genes involved in flare formation may be essential. Therefore, we generated a collection of 1,500 conditional mutants that were viable at 23°C but not at 34°C and screened them for mutants that arrested in mitosis at 34°C with a round nucleus (Figure 1A). We found “no-flare” (nf) mutants in the yeast polo kinase gene *CDC5* and in the lipid synthesis genes *FAS1*, *FAS2*, and *ACC1*. The *cdc5-nf* mutant is the focus of this study.

The *cdc5-nf* allele carries a mutation, E178K, in a highly conserved residue within the kinase domain (Figure S1A available online). Less than 10% of nocodazole-treated, mitotically arrested *cdc5-nf* cells possessed a nuclear flare, compared to around 90% of wild-type (WT) cells (Figures 1A and 1B). Expression of WT *CDC5* from a *CEN* plasmid restores the flared nuclear phenotype (Figure 1B). A similar result was observed when a mitotic arrest was induced by inactivating an anaphase-promoting complex subunit, Cdc16 [6] (Figures S1B and S1C). As with previously isolated *cdc5* mutant alleles [7–9], the terminal phenotype of *cdc5-nf* at 34°C was a telophase arrest (Figures 1A and S2D) due to a requirement for Cdc5 in mitotic exit. In mitotically arrested cells, Cdc5 accumulated in the nucleoplasm (Figures 1C and S1D) and spindle pole bodies [10] and was occasionally visible as a fine thread through the nucleolus, possibly due to its association with the rDNA array [11]. As expected, *cdc5-nf* did not affect nuclear remodeling following exposure to α factor mating pheromone (Figures S1E and S1F), because Cdc5 is not expressed during G1 [12].

The no-flare phenotype was not specific to *cdc5-nf*, as other *cdc5* alleles that were inviable at 34°C, *cdc5-1* and *cdc5-66* [13] (Figures S1A and S2A), also exhibited a mitotic flare formation defect (Figure S2B). The severity of the no-flare phenotype was inversely proportional to the Cdc5 activity at 34°C, as measured by the degree of rDNA condensation (Figures 1D and 1E). Depletion of Cdc5 using an auxin-induced *cdc5-degron* allele [14] (Figures S2C and S2D) also resulted in a mitotic no-flare phenotype (Figure S2E). These data suggest that the no-flare nuclear phenotype seen in the *cdc5-nf* strain is due to reduced Cdc5 activity.

Cdc5 Is Required for Maintenance of the Nuclear Flare

When mitotically arrested *cdc5-nf* cells were allowed to form flares at 23°C and then shifted to 34°C, the number of cells with flared nuclei dropped precipitously (Figure 1F). The flares that did persist in *cdc5-nf* cells tended to be collapsed (a smaller loop than at time 0) or flattened onto the DAPI mass (Figures 1G and S2F). Based on their rate of appearance, “bulged” nuclei, where the nucleolus only slightly protrudes away from the DAPI mass, may be an intermediate step between a flared and round nucleus (Figures 1G and S2F). Thus, Cdc5 is required for flare maintenance during a mitotic arrest.

The Effect of Cdc5 on Nuclear Morphology Is Not Imposed through FEAR, MEN, or rDNA Condensation

Cdc5 has been implicated in multiple mitotic processes, including FEAR (Cdc fourteen early anaphase release), MEN

*Correspondence: ornac@helix.nih.gov



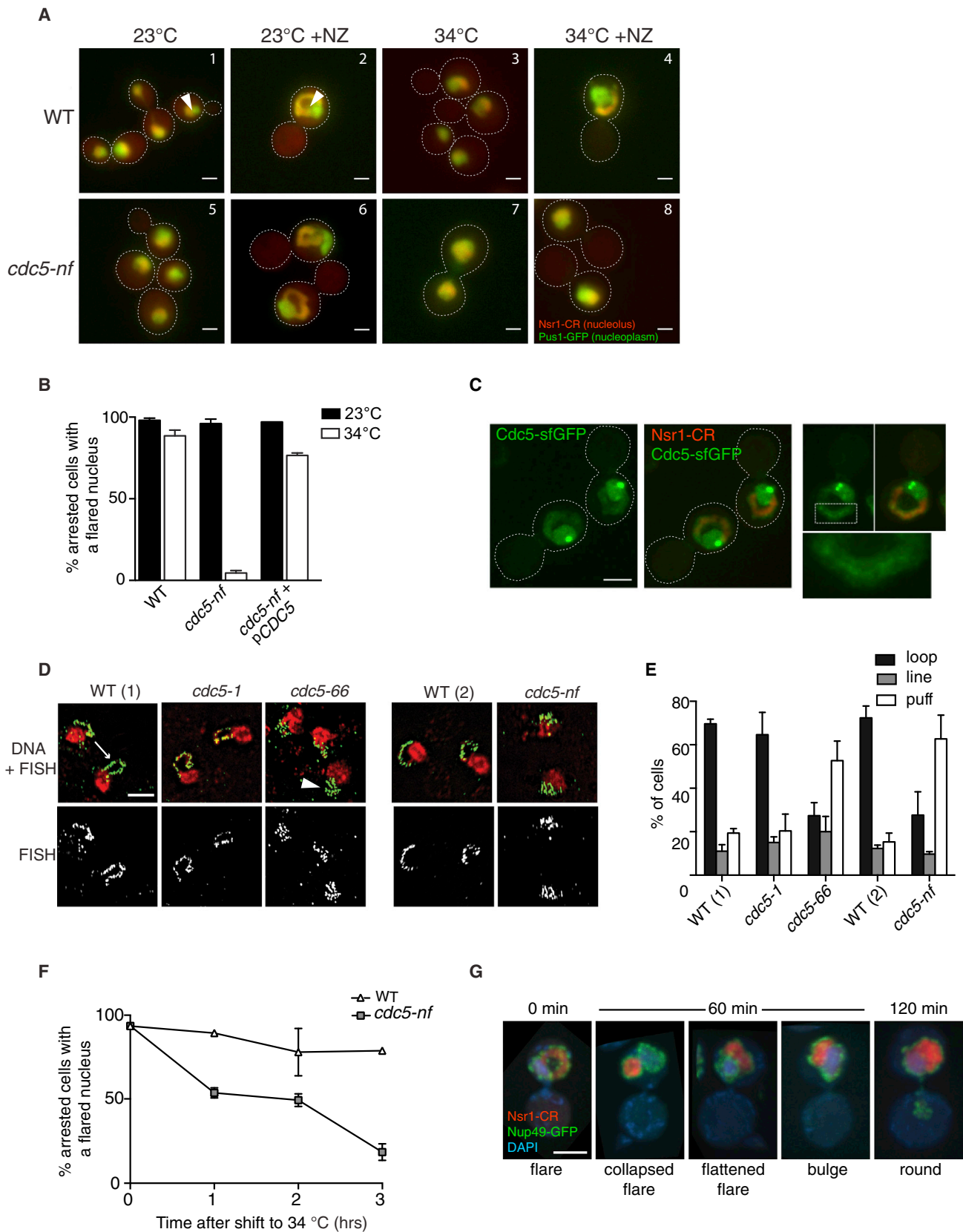


Figure 1. Cdc5 Affects Nuclear Morphology during a Mitotic Arrest

(A) Merged fluorescence images of fixed mitotically arrested WT (top row) and *cdc5-nf* (bottom row) cells. The nucleoplasm is marked with Pus1-GFP (green) and the nucleolus with Nsr1-mCherry (red). A nuclear flare containing the nucleolus forms in WT cells during a mitotic arrest induced by nocodazole at both

(legend continued on next page)

(mitotic exit network) [15, 16], and rDNA condensation [17]. All mitotically arrested FEAR and MEN mutants tested displayed a flared nuclear phenotype indistinguishable from WT (Figures S2G and S2H), indicating that flare formation is independent of FEAR and MEN.

Given the inverse correlation between Cdc5 activity and the severity of the no-flare phenotype noted above (Figures 1D, 1E, and S2B), it was possible that flare formation was dependent on rDNA condensation. If that were the case, then disruption of rDNA condensation by other means, such as condensin inactivation [18], should also result in a no-flare phenotype. However, condensin mutants (*brn1-9* [19] and *ycs4-1* [20]) that exhibit rDNA condensation defects at 34°C (Figures 2A and 2B) still form flares when arrested in mitosis at 34°C (Figures 2C, 2D, and S3), demonstrating that rDNA condensation is not required for flare formation. Condensin mutants, however, displayed wider and less extended flares than those seen in WT cells (Figures 2C and S3). Thus, although flares are present in mutants defective in rDNA condensation, the shape of the flare may be affected by the structure of the rDNA/nucleolus.

Further evidence that rDNA condensation is not required for flare formation came from a strain in which the rDNA was deleted and replaced by a plasmid carrying a single rDNA repeat [21]. As a result, the nucleolus forms a “dot” rather than the typical crescent shape (Figure 2E). This strain grew poorly and exhibited jagged-edged nuclei (Figure 2E). However, flared nuclei were observed in 70% ± 7% of mitotically arrested cells compared to only 21% ± 1% of interphase cells (Figure 2E). The presence of NE extensions during interphase may be due to the poor growth of this strain. Nonetheless, mitotic flares can form independent of rDNA.

Finally, we examined whether Cdc5 affects nuclear morphology through the attachment of rDNA to the NE [22]. If this anchoring allowed flare formation, then mutations that lead to the detachment of the rDNA from the NE should produce a no-flare phenotype. However, such mutants, including *heh1Δ*, *csml1Δ*, *lrs4Δ*, and *nur1Δ* [22], exhibited flared nuclei when arrested in mitosis (Figure 2F). Conversely, if the rDNA had to detach from the NE for a flare to form, and Cdc5 were required for this detachment, then combining *cdc5-nf* and rDNA detachment mutants should give rise to flared nuclei, because the rDNA is constitutively detached from the NE. However, deletion of rDNA attachment genes in a *cdc5-nf* background did not restore flare formation (Figure 2F). Therefore, Cdc5 is not affecting nuclear morphology via rDNA condensation or its NE attachment.

Cdc5 Confines NE Expansion to the Nucleolar Region during a Mitotic Arrest

Because flare formation involves NE expansion [4], we imagine that in the mitotically arrested *cdc5-nf* mutant either the NE does not expand or the NE does expand but the added nuclear membrane is distributed uniformly throughout the NE, resulting in isometric expansion. To distinguish between these two possibilities, NE expansion during a mitotic arrest was measured using soft X-ray tomography. WT and *cdc5-nf* cells were staged in G1 and released into media containing nocodazole (NZ) at 34°C, and NE expansion was followed as cells progressed toward a mitotic arrest (Figure 3A), using cell volume as a proxy for cell-cycle progression.

Tomographic reconstructions (Figure 3B) revealed that, as seen previously by fluorescence, very few nuclei (9%) in large budded *cdc5-nf* cells (cell volume >140 μm³) were flared, whereas 95% of large budded WT cells contained flared nuclei. However, the nuclear surface areas in both WT and *cdc5-nf* cells increased at the same rate (i.e., the amount of surface area added as a function of cell volume) (Figure 3C), demonstrating that *cdc5-nf* nuclei are expanding isometrically. This suggests that Cdc5 is required to designate the nucleolus as the site of NE expansion during a mitotic arrest. Interestingly, mutant cells had the same nuclear:cell volume ratio as WT cells, despite their different morphologies (Figure 3D). Nuclear:cell volume ratio was shown previously to be constant [23, 24], although the underlying mechanism and the functional importance of this ratio are not known. We speculate that flare formation allows the cell to expand its nuclear surface area without altering its nuclear volume, thus maintaining a constant nuclear:cell volume ratio and limiting the disruption to the space in which the bulk of the DNA resides. The isometric expansion of the *cdc5-nf* nucleus likely increases the space occupied by the chromosomes, the consequences of which are currently unknown.

Cdc5 Allows Transient NE Expansion at the Nucleolus during Uninterrupted Mitosis

To characterize NE dynamics in cycling cells, WT cells were imaged every 5 min until they completed anaphase. Small budded cells (Figure 4A, 0 min) had a spherical nucleus, but in 10 out of 16 time courses a small expansion of the nucleus in the nucleolar region was visible prior to anaphase (Figure 4A, 15 min, white arrowhead; Figure S4B). This expansion, or “miniflare,” was defined as an expansion of an interphase nucleus that disrupts the continuity of the normal round nuclear shape

23°C and 34°C (panels 2 and 4) and in *cdc5-nf* cells at 23°C (panel 6). Nuclei of *cdc5-nf* cells are round at 34°C in the presence of NZ (panel 8). In the absence of NZ, *cdc5-nf* cells arrest in late telophase at 34°C (panel 7; Figure S2E). White arrowheads indicate the interface between the nucleolus and nucleoplasm (panels 1 and 2). The scale bars represent 2 μm.

(B) Quantification of phenotypes of NZ-treated cells shown in (A). For each condition, n = 100 in at least two biological replicates.

(C) Cdc5 nuclear localization during a mitotic arrest. WT cells expressing Cdc5-sfGFP and Nsr1-mCherry (nucleolar marker) were arrested in NZ at 30°C and imaged using fluorescence confocal microscopy. Bright green spots are at the spindle pole bodies. The area contained in the white dashed box (right panels) is expanded in the bottom-right panel to show a thin line of Cdc5-sfGFP within the nucleolar flare. See Figure S1D for Cdc5-sfGFP localization in asynchronous cells. The scale bar represents 3 μm.

(D) Images from fluorescence in situ hybridization (FISH) using a probe for rDNA in WT and *cdc5* mutants. Cells were arrested in NZ at 34°C for 150 min. WT (1) is isogenic to strains *cdc5-1* and *cdc5-66*, whereas WT (2) is isogenic to strain *cdc5-nf*. WT cells arrested in mitosis typically exhibit an rDNA “loop” (arrow), whereas mutants defective in rDNA condensation exhibit amorphous structures referred to as “puff” (arrowhead) [31]. The scale bar represents 5 μm.

(E) Quantification of rDNA phenotypes of *cdc5* mutants from FISH described in (D).

(F) Cdc5 is required for the maintenance of a nuclear flare. *cdc5-nf* and WT cells were arrested in mitosis at 23°C to allow flare formation and then shifted to 34°C. Samples were taken at the indicated time points. For each time point, n = 100 in at least three biological replicates. See also Figure S2F.

(G) Images of *cdc5-nf* cells from the experiment in Figure S2F showing examples of the collapse and eventual loss of nuclear flares upon the inactivation of Cdc5. NZ-arrested WT and *cdc5-nf* cells were shifted from 23°C to 34°C. Cells were fixed every 30 min and imaged by confocal fluorescence microscopy. The images shown are from 60 and 120 min. The NE is marked with Nup49-GFP (green), the nucleolus with Nsr1-mCherry (red), and DNA with DAPI (blue). The scale bar represents 3 μm.

Error bars in all panels indicate SD.

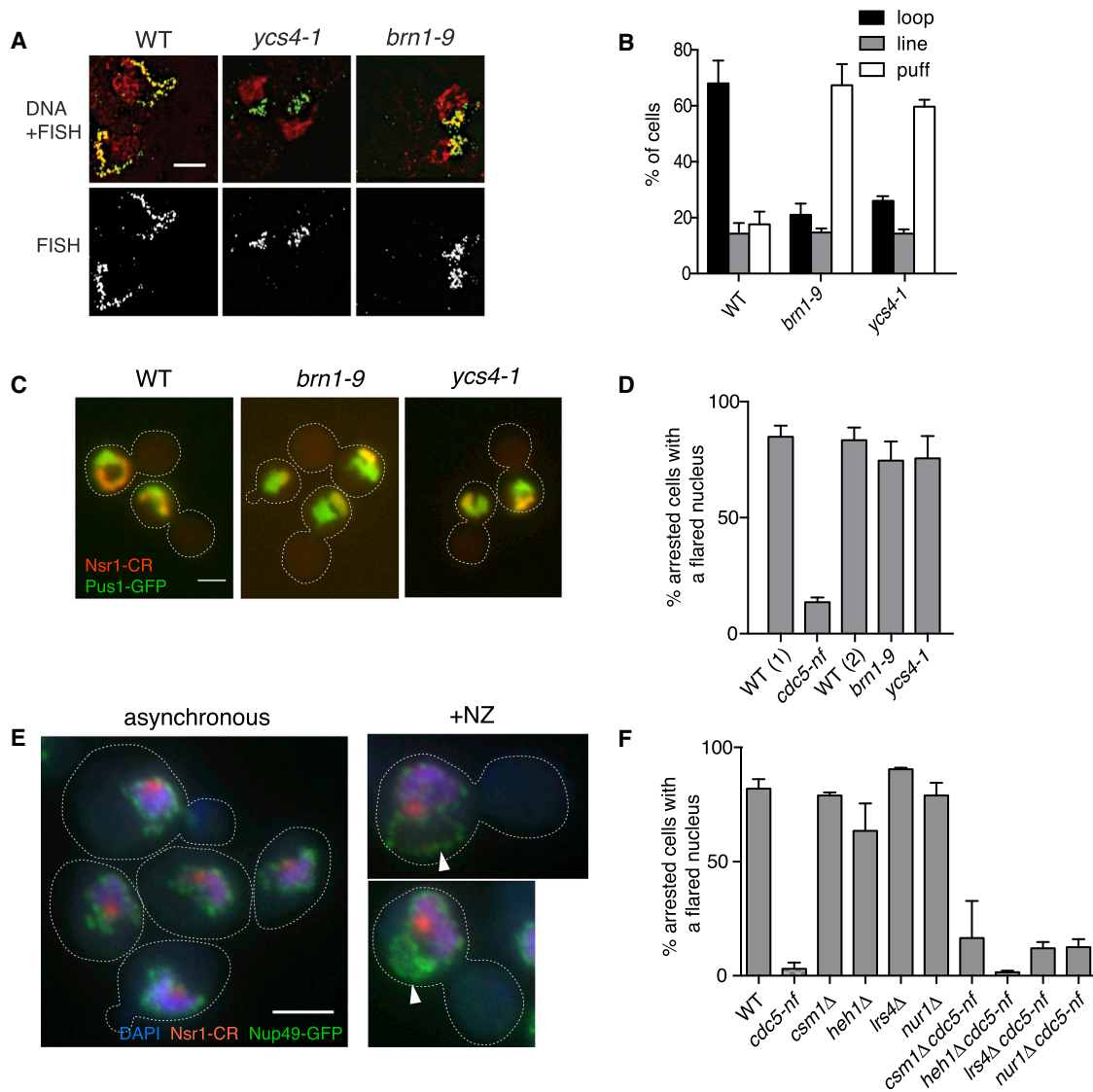


Figure 2. Cdc5 Is Not Affecting Nuclear Morphology through rDNA Condensation or Attachment to the NE

(A) Images from FISH using a probe for rDNA in condensin mutants. Cells were arrested in NZ at 34°C for 150 min. rDNA is shown in green; DNA is in red. The scale bar represents 5 μm.

(B) Quantification of rDNA phenotypes of condensin mutants from FISH described in (A).

(C) Merged fluorescence images of WT and condensin mutant cells arrested in NZ at 34°C. The nucleoplasm is marked with Pus1-GFP (green) and the nucleolus with Nsr1-mCherry (red). The scale bar represents 3 μm. See also Figure S3.

(D) Quantification of nuclear phenotypes for the NZ-arrested condensin mutant experiment shown in (C). WT (1) is isogenic to strain *cdc5-nf*, whereas WT (2) is isogenic to strains *brn1-9* and *ycs4-1*.

(E) Merged fluorescence images of asynchronous and NZ-arrested cells in a strain where the chromosomal rDNA was replaced by a single plasmid-borne copy of the rDNA. White arrowheads indicate nuclear flares. The nuclear pore subunit Nup49-GFP marks the NE (green), Nsr1-mCherry marks the “dot” nucleolus (red spot), and DAPI-stained DNA is shown in blue. The scale bar represents 3 μm.

(F) Quantification of nuclear phenotypes of NZ-arrested rDNA-NE detachment mutants alone and in combination with the *cdc5-nf* allele.

For (B), (D), and (F) for each condition, n = 100 in each of at least two biological replicates. Error bars in all panels indicate SD.

(Figure 4B). It always occurred at the nucleolar region and was more prevalent in cells with a larger bud:mother size ratio, shortly before entering anaphase (Figures 4C and 4D).

As a more objective measure of the formation of a miniflare, the sphericity of interphase nuclei was determined. The sphericity of a given object is the ratio between the surface area of a sphere with the same volume as that object and the surface area of the object itself [25]. Thus, the sphericity of a sphere would equal 1, and perturbations to the shape of a sphere, which would increase its surface area, would result in

sphericity values that are less than 1. For example, the sphericity of the elongated nuclei in α factor-arrested cells (Figure S1E) is around 0.8. We found that nuclei that did not have a miniflare had an average sphericity value of 0.95, whereas the average sphericity of nuclei that were designated as having a miniflare was 0.88 (Figures S4A and S4B).

We next determined whether these miniflares were dependent on Cdc5 using the auxin-inducible *cdc5-deg* strain. Both the *cdc5-deg* and control strains were grown at 23°C to mid-log phase and exposed to auxin. Interphase cells

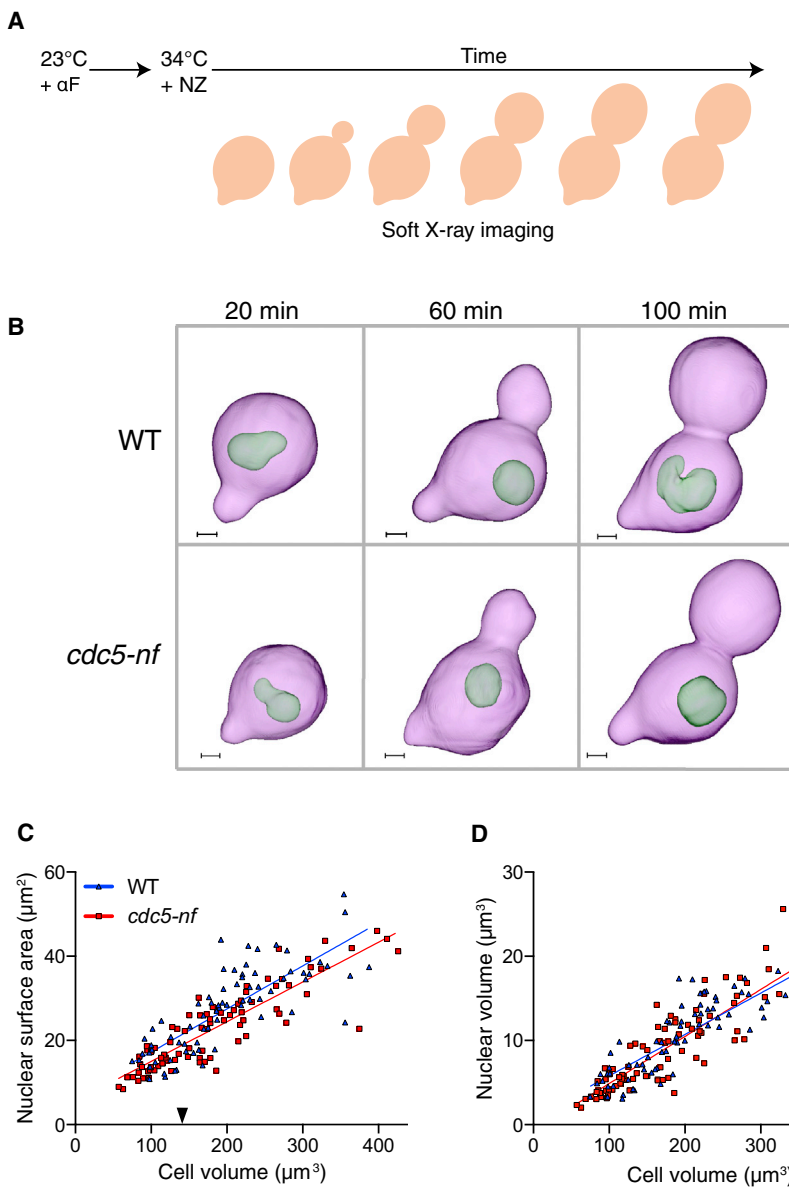


Figure 3. Nuclei of *cdc5-nf* Cells Expand Isometrically during a Mitotic Arrest

(A) Outline of the experiment. WT and *cdc5-nf* cells were arrested in G1 with α factor and then released into NZ at 34°C. Samples were taken every 20 min and processed for soft X-ray imaging.

(B) Surface-rendered views of the cell (pink) and nucleus (pale green) after segmentation of 3D reconstructions of WT and *cdc5-nf* cells from the experiment described in (A). The scale bars represent 1 μ m.

(C) Quantification of nuclear surface areas as a function of cell size of WT and *cdc5-nf* cells ($n = 74$ and 86 , respectively). Nuclear flares begin to appear in cells of approximately $140 \mu\text{m}^3$ (black triangle). Linear regressions were calculated using GraphPad Prism ($R^2_{WT} = 0.633$, $R^2_{cdc5-nf} = 0.774$). There is no significant difference between the slope of the line describing the increase in nuclear surface areas in WT and *cdc5-nf* ($p = 0.44$, ANCOVA [analysis of covariance]). Nuclei of WT cells have a slightly greater surface area than nuclei of *cdc5-nf* across all cell sizes ($p = 0.0006$, ANCOVA).

(D) Quantification of nuclear volumes as a function of cell size of the same cells as (C). There is no significant difference between nuclear volumes in WT ($R^2 = 0.677$) and *cdc5-nf* ($R^2 = 0.762$) across all cell sizes ($p = 0.48$, ANCOVA).

were analyzed after 2 hr in the presence of auxin, when $\sim 50\%$ of the *cdc5-degron* cells had arrested in telophase and Cdc5 levels were significantly reduced (Figure S2C). Miniflares were visible in 36% of budded control cells but only in 18% of budded Cdc5-depleted cells (Figure 4C), and this difference was even more pronounced in cells with larger buds (bud:mother size ratio >0.66) (Figure 4D). Moreover, the sphericity of nuclei in the absence of Cdc5 was significantly greater than the sphericity of the control cells (Figure S4A). Thus, Cdc5 plays a role in regulating NE expansion not only during a mitotic delay but also in unperturbed cycling cells.

Our studies uncovered a new role for Cdc5 in the compartmentalization of the yeast NE. Cdc5 regulates nuclear morphology by designating the NE adjacent to the nucleolus as the site of NE expansion in both mitotically arrested and cycling cells. By coupling Cdc5, which is active in later stages of the cell cycle, to NE expansion, the cell can expand its nucleus isometrically during G1 and S phase and confine NE expansion to the nucleolar region early in mitosis and during a mitotic delay. It is likely that when mitosis is delayed and lipid

synthesis continues unabated [4], the miniflare develops into a full-sized flare. How might Cdc5 affect NE distribution? Although the precise mechanism is not known, it is independent of Cdc5's roles in the FEAR pathway, the MEN, and rDNA condensation. The confinement of the flare or miniflare to the NE adjacent to the nucleolus may prevent disruption to the rest of the nucleus, where the majority of the chromosomes reside. Once released from a mitotic arrest, the nonflared nuclei of *cdc5-nf* are able to complete anaphase without

arrest is delayed compared to WT, as judged by their initial rate of spindle elongation (data not shown). Whether this is due to the altered nuclear shape or to another Cdc5-related function awaits the identification of the relevant Cdc5 target(s) involved in flare formation.

The regulation of NE expansion is of great significance to the study of aging and cancer, where nuclear size and shape are often disrupted. Although the role of Cdc5 in flare formation may be specific to closed mitosis, the relevant target(s) of this conserved kinase may play a role in membrane dynamics in higher eukaryotes. The mammalian polo kinase (Plk1) has known functions in membrane restructuring during mitosis, playing a role in Golgi breakdown [26] and in coordinating abscission with other mitotic events during cytokinesis [27]. Plk1 has also been proposed to affect NE breakdown [28, 29]. In mammalian cells, depletion of Plk1 leads to altered nuclear morphology [30], a phenotype that has been attributed to chromosome missegregation in the absence of Plk1. Our findings linking yeast polo kinase to NE expansion indicate that Plk1 may have a more direct role in regulating nuclear shape.

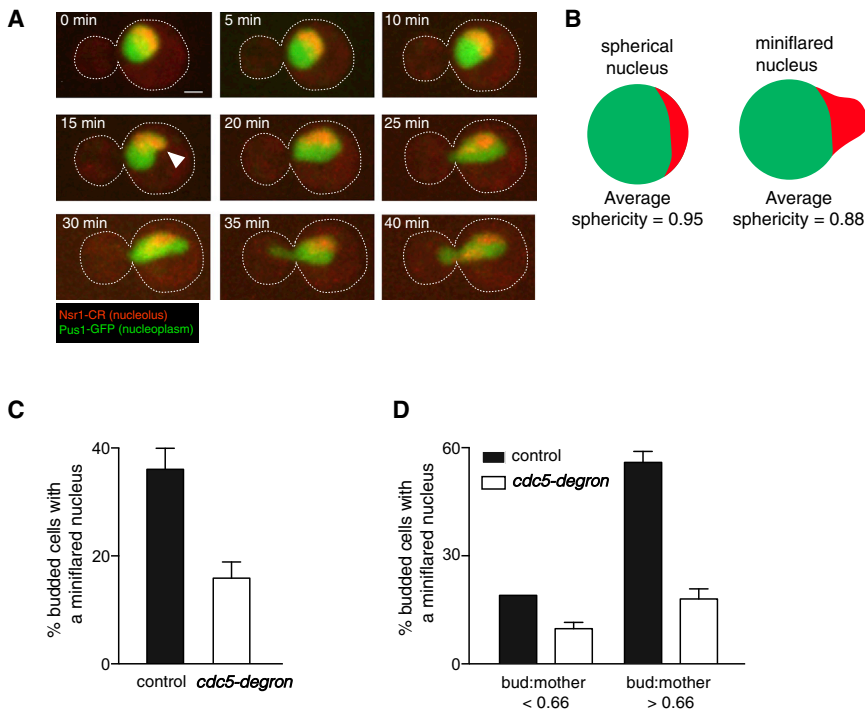


Figure 4. Cdc5 Allows NE Expansion at the Nucleolar Region during an Uninterrupted Mitosis
(A) Images from a time course of a WT cell progressing from a small budded stage into anaphase. The nucleoplasm is marked with Pus1-GFP (green) and the nucleolus with Nsr1-mCherry (red). Images shown are maximum projections of merged fluorescence confocal images. A miniflare (white arrowhead) is visible at 15 min. The scale bar represents 1 μ m.
(B) A miniflare disrupts the spherical surface of the nucleus (green), specifically at the site of the nucleolus (red). Sphericity data are from Figure S4A.
(C) Miniflares are Cdc5 dependent. Quantification of the frequency of miniflares in a control strain and *cdc5-degroun* cells. Fixed log-phase cells were imaged by fluorescence confocal microscopy, and nuclear phenotypes of all budded cells were scored. The frequency of miniflares in budded cells was lower in the *cdc5-degroun* strain ($p < 0.0001$, Fisher's exact test).
(D) Data from (C) divided into categories by bud: mother cell-size ratio. For bud:mother < 0.66, $n = 79$ and 66 for WT and *cdc5-degroun* cells, respectively. For bud:mother > 0.66, $n = 69$ and 134 for WT and *cdc5-degroun* cells, respectively. The frequency of miniflares in cells with larger buds is significantly lower in the *cdc5-degroun* strain ($p < 0.0001$, Fisher's exact test). The difference in frequency of miniflares in cells with small buds is not statistically significant ($p = 0.1665$, Fisher's exact test).
Error bars in all panels represent SD.

Supplemental Information

Supplemental Information includes Supplemental Experimental Procedures, four figures, and one table and can be found with this article online at <http://dx.doi.org/10.1016/j.cub.2014.10.029>.

Acknowledgments

We thank D. Reynolds, A. Hoyt, T. Eng, D. Koshland, A. Amon, S. Lacefield, and J. Diffley for yeast strains and plasmids and M. Lichten, W. Prinz, F. Chang, and members of the O.C.-F. laboratory for discussions on the manuscript. A.D.W., C.K.M., E.S.D., and O.C.-F. are funded by an intramural National Institute of Diabetes and Digestive and Kidney Diseases grant. C.A.L., B.P.C., and E.A.S. are funded by the National Institute of General Medical Science of the NIH (P41GM103445) and the U.S. Department of Energy, Office of Biological and Environmental Research (DE-AC02-05CH11231). Research in D.D.'s laboratory is supported by the Canadian Institutes of Health Research (MOP 82912 and MOP 136788). D.D. is a recipient of a Tier II Canada Research Chair in Cell Cycle Regulation and Genomic Integrity.

Received: May 16, 2014

Revised: September 23, 2014

Accepted: October 9, 2014

Published: November 20, 2014

References

- Chow, K.-H., Factor, R.E., and Ullman, K.S. (2012). The nuclear envelope environment and its cancer connections. *Nat. Rev. Cancer* 12, 196–209.
- Scaffidi, P., and Misteli, T. (2006). Lamin A-dependent nuclear defects in human aging. *Science* 312, 1059–1063.
- Kutay, U., and Hetzer, M.W. (2008). Reorganization of the nuclear envelope during open mitosis. *Curr. Opin. Cell Biol.* 20, 669–677.
- Witkin, K.L., Chong, Y., Shao, S., Webster, M.T., Lahiri, S., Walters, A.D., Lee, B., Koh, J.L.Y., Prinz, W.A., Andrews, B.J., and Cohen-Fix, O. (2012). The budding yeast nuclear envelope adjacent to the nucleolus serves as a membrane sink during mitotic delay. *Curr. Biol.* 22, 1128–1133.
- Archambault, V., and Glover, D.M. (2009). Polo-like kinases: conservation and divergence in their functions and regulation. *Nat. Rev. Mol. Cell Biol.* 10, 265–275.
- Irriger, S., Piatti, S., Michaelis, C., and Nasmyth, K. (1995). Genes involved in sister chromatid separation are needed for B-type cyclin proteolysis in budding yeast. *Cell* 81, 269–278.
- Jaspersen, S.L., Charles, J.F., Tinker-Kulberg, R.L., and Morgan, D.O. (1998). A late mitotic regulatory network controlling cyclin destruction in *Saccharomyces cerevisiae*. *Mol. Biol. Cell* 9, 2803–2817.
- Lee, S.E., Frenz, L.M., Wells, N.J., Johnson, A.L., and Johnston, L.H. (2001). Order of function of the budding-yeast mitotic exit-network proteins Tem1, Cdc15, Mob1, Bdf2, and Cdc5. *Curr. Biol.* 11, 784–788.
- Visintin, R., Craig, K., Hwang, E.S., Prinz, S., Tyers, M., and Amon, A. (1998). The phosphatase Cdc14 triggers mitotic exit by reversal of Cdk-dependent phosphorylation. *Mol. Cell* 2, 709–718.
- Song, S., Grenfell, T.Z., Garfield, S., Erikson, R.L., and Lee, K.S. (2000). Essential function of the polo box of Cdc5 in subcellular localization and induction of cytokinetic structures. *Mol. Cell Biol.* 20, 286–298.
- Rossio, V., Galati, E., Ferrari, M., Pelliccioli, A., Sutani, T., Shirahige, K., Lucchini, G., and Piatti, S. (2010). The RSC chromatin-remodeling complex influences mitotic exit and adaptation to the spindle assembly checkpoint by controlling the Cdc14 phosphatase. *J. Cell Biol.* 191, 981–997.
- Shirayama, M., Zachariae, W., Ciosk, R., and Nasmyth, K. (1998). The Polo-like kinase Cdc5p and the WD-repeat protein Cdc20p/fizzy are regulators and substrates of the anaphase promoting complex in *Saccharomyces cerevisiae*. *EMBO J.* 17, 1336–1349.
- Ratsima, H., Ladouceur, A.-M., Pascariu, M., Sauvé, V., Salloum, Z., Maddox, P.S., and D'Amours, D. (2011). Independent modulation of the kinase and polo-box activities of Cdc5 protein unravels unique roles in the maintenance of genome stability. *Proc. Natl. Acad. Sci. USA* 108, E914–E923.
- Nishimura, K., Fukagawa, T., Takisawa, H., Kakimoto, T., and Kanemaki, M. (2009). An auxin-based degron system for the rapid depletion of proteins in nonplant cells. *Nat. Methods* 6, 917–922.
- Rock, J.M., and Amon, A. (2009). The FEAR network. *Curr. Biol.* 19, R1063–R1068.
- Segal, M. (2011). Mitotic exit control: a space and time odyssey. *Curr. Biol.* 21, R857–R859.

17. St-Pierre, J., Douziech, M., Bazile, F., Pascariu, M., Bonneil, E., Sauvé, V., Ratsima, H., and D'Amours, D. (2009). Polo kinase regulates mitotic chromosome condensation by hyperactivation of condensin DNA supercoiling activity. *Mol. Cell* *34*, 416–426.
18. Freeman, L., Aragon-Alcaide, L., and Strunnikov, A. (2000). The condensin complex governs chromosome condensation and mitotic transmission of rDNA. *J. Cell Biol.* *149*, 811–824.
19. Lavoie, B.D., Tuffo, K.M., Oh, S., Koshland, D., and Holm, C. (2000). Mitotic chromosome condensation requires Brn1p, the yeast homologue of Barren. *Mol. Biol. Cell* *11*, 1293–1304.
20. Biggins, S., Bhalla, N., Chang, A., Smith, D.L., and Murray, A.W. (2001). Genes involved in sister chromatid separation and segregation in the budding yeast *Saccharomyces cerevisiae*. *Genetics* *159*, 453–470.
21. Wai, H.H., Vu, L., Oakes, M., and Nomura, M. (2000). Complete deletion of yeast chromosomal rDNA repeats and integration of a new rDNA repeat: use of rDNA deletion strains for functional analysis of rDNA promoter elements in vivo. *Nucleic Acids Res.* *28*, 3524–3534.
22. Mekhail, K., Seebacher, J., Gygi, S.P., and Moazed, D. (2008). Role for perinuclear chromosome tethering in maintenance of genome stability. *Nature* *456*, 667–670.
23. Jorgensen, P., Edgington, N.P., Schneider, B.L., Rupes, I., Tyers, M., and Fitcher, B. (2007). The size of the nucleus increases as yeast cells grow. *Mol. Biol. Cell* *18*, 3523–3532.
24. Neumann, F.R., and Nurse, P. (2007). Nuclear size control in fission yeast. *J. Cell Biol.* *179*, 593–600.
25. Wadell, H. (1935). Volume, shape, and roundness of quartz particles. *J. Geol.* *43*, 250–280.
26. Lin, C.Y., Madsen, M.L., Yarm, F.R., Jang, Y.J., Liu, X., and Erikson, R.L. (2000). Peripheral Golgi protein GRASP65 is a target of mitotic polo-like kinase (Plk) and Cdc2. *Proc. Natl. Acad. Sci. USA* *97*, 12589–12594.
27. Chen, C.-T., Hehnl, H., and Doxsey, S.J. (2012). Orchestrating vesicle transport, ESCRTs and kinase surveillance during abscission. *Nat. Rev. Mol. Cell Biol.* *13*, 483–488.
28. Li, H., Liu, X.S., Yang, X., Song, B., Wang, Y., and Liu, X. (2010). Polo-like kinase 1 phosphorylation of p150Glued facilitates nuclear envelope breakdown during prophase. *Proc. Natl. Acad. Sci. USA* *107*, 14633–14638.
29. Laurell, E., Beck, K., Krupina, K., Theerthagiri, G., Bodenmiller, B., Horvath, P., Aebersold, R., Antonin, W., and Kutay, U. (2011). Phosphorylation of Nup98 by multiple kinases is crucial for NPC disassembly during mitotic entry. *Cell* *144*, 539–550.
30. Lera, R.F., and Burkard, M.E. (2012). High mitotic activity of Polo-like kinase 1 is required for chromosome segregation and genomic integrity in human epithelial cells. *J. Biol. Chem.* *287*, 42812–42825.
31. Lavoie, B.D., Hogan, E., and Koshland, D. (2004). In vivo requirements for rDNA chromosome condensation reveal two cell-cycle-regulated pathways for mitotic chromosome folding. *Genes Dev.* *18*, 76–87.